http://dx.doi.org/10.5012/bkcs.2012.33.8.2694

Fabrication and Thermal Oxidation of ZnO Nanofibers Prepared *via* Electrospinning Technique

Jeong-Ha Baek, Juyun Park, Jisoo Kang,† Don Kim, Sung-Wi Koh,‡ and Yong-Cheol Kang*

*Department of Chemistry, Pukyong National University, Busan 608-737, Korea. *E-mail: yckang@pknu.ac.kr*
†Department of Chemistry and Biochemistry, University of California at Los Angeles, Los Angeles, CA, 90024, USA
‡Department of Mechanical System Engineering, Pukyong National University, Busan 608-739, Korea
Received April 17, 2012, Accepted May 18, 2012

Materials on the scale of nanoscale have widely been used as research topics because of their interesting characteristics and aspects they bring into the field. Out of the many metal oxides, zinc oxide (ZnO) was chosen to be fabricated as nanofibers using the electrospinning method for potential uses of solar cells and sensors. After ZnO nanofibers were obtained, calcination temperature effects on the ZnO nanofibers were studied and reported here. The results of scanning electron microscopy (SEM) revealed that the aggregation of the ZnO nanofibers progressed by calcination. X-ray diffraction (XRD) study showed the hcp ZnO structure was enhanced by calcination at 873 and 1173 K. Transmission electron microscopy (TEM) confirmed the crystallinity of the calcined ZnO nanofibers. X-ray photoelectron spectroscopy (XPS) verified the thermal oxidation of Zn species by calcination in the nanofibers. These techniques have helped us deduce the facts that the diameter of ZnO increases as the calcination temperature was raised; the process of calcination affects the crystallinity of ZnO nanofibers, and the thermal oxidation of Zn species was observed as the calcination temperature was raised.

Key Words : Zn oxide nanofibers, XPS, Electrospinning, XRD

Introduction

One-dimensional (1D) nano-materials with high surface to volume ratio have attracted attention because of their exceptional chemical and physical properties and various applications.[1-3] There are many kinds of 1D nanostructures such as nano-belts,[4] nanoneedles,[5] nanorods,[6] nanorings,[7] nanowires,[8] nanotubes,[9] and nanofibers.[10] These materials can be produced using various methods such as the sol-gel process,[11] sputtering,[12] spray pyrolysis,[13] hydrothermal,[14] electrospinning,[15,16] and electrochemical deposition.[17] Among these techniques pertaining to the 1D nano-materials, the electrospinning method is more versatile and convenient than the other processes for synthesizing organic and inorganic nanofibers.[1,18,19] The nanofibers have many industrial applications used in a variety of fields such as sensors, filtration, biological cells, electronic devices, and protective clothing, *etc*.[19,20]

Among the 1D transition metal oxides, ZnO has some distinct characteristics such as being non-toxic, having a wide band gap of 3.37 eV at room temperature, having a largely excited binding energy, being inexpensive, and containing photochemical properties. Moreover the 1D nano-sized ZnO is suitable candidate for solar cells, sensors, optoelectronics devices due to its transparent and conductive property.[1,21,22]

Recently, ZnO nanofibers with high crystallinity have been successfully fabricated using the electrospinning process. Despite the unique properties of ZnO, research on the influence of the oxidation states of ZnO dependent on the calcined temperature is still lacking.

Therefore, we studied ZnO nanofibers calcined at different temperatures, which characterized by scanning electron microscopy (SEM), X-ray diffraction (XRD), transmission electron microscopy (TEM), and X-ray photoelectron spectroscopy (XPS)

Experimental

To fabricate 1D nanostructure zinc oxide (ZnO) nanofibers, the electrospinning process was adopted. Two separate solutions, one containing zinc acetate ($Zn(CH_3COO)_2 \cdot 2H_2O$, MW: 219.51, Junsei Chemical) and the other containing polyvinylpyrrolidone (PVP, $(C_6H_9NO)_x$, MW: ~1,300,000, Sigma Aldrich) were prepared as precursor solutions. The PVP solution was made by dissolving 0.77 g of PVP into 13 mL of ethanol (EtOH, 99.9%) and the other solution was made by having 3 g of zinc acetate being added into 10 mL of distilled water. Both solutions were stirred for 5 hrs at room temperature separately. After this step, 1.0 mL of the zinc acetate solution was transferred to the PVP-EtOH solution then the mixed solution was vigorously stirred for 5 hrs at rt. The Zn/PVP solution had a reading of 42.65 cP of viscosity measured with a viscometer (SU-10, A&D). The mixed solution was used as a precursor for electrospinning. The Zn/PVP solution was loaded to a plastic syringe (10 mL) equipped with a flat tip of 21-gauge stainless needle. The syringe was placed on a syringe pump (KDS scientific) which was adjusted to 16 μL/min of feeding rate. A high voltage of 10.3 kV was applied to the metal needle tip. And

an electrically grounded drum collector was covered with aluminum foil and rotated at 100 revolutions per minute. The working distance between the drum collector and the needle tip was fixed at 15 cm during the electrospinning process. The electrospun Zn/PVP nanofibers were initially dried to evaporate the residual organic solvent in the nanofiber. During the drying process, the temperature was kept at 353 K with a tube furnace (DTF-40300-12T, Daeheung Scientific Co.) for 5 hrs in ambient environment. Then the dried ZnO nanofibers (Zn-rt) were calcined at 873 and 1173 K based on the previous research of thermogravimetric analysis.[23] Hereafter, the ZnO nanofibers calcined at 873 and 1173 K are named as Zn-873 and Zn-1173, respectively. Surface morphologies of the ZnO nanofibers were investigated using FE-SEM (JEOL, JSM-6700F). And the phase and crystallinity of ZnO nanofibers were checked by XRD (PHILIPS, X'Pert-MPD System), and TEM (JEOL, JEM-2010). To characterize the chemical nature of the ZnO nanofibers, XPS (VG, EscaLab MK II) was performed.

Results and Discussion

SEM Analysis. Figure 1 shows the SEM images of the morphologies of Zn-rt, Zn-873, and Zn-1173. As shown in Figure 1(a), Zn-rt was uniform, smooth, and continuous nanofibers which have 149 (± 2) nm of average diameter were formed. Figures 1(b) and (c) show that post-calcined ZnO porous nanomats of Zn-873 and Zn-1173 have average diameters of 57 (± 1) nm and 207 (± 6) nm, respectively. As the calcination temperature increased to 873 K, the PVP in/on Zn-rt nanofibers decomposed and evaporated, so ZnO crystals emerged on the surface, which has a coarse surface and decreased diameter. After calcination at 1173 K for 5 hrs, the ZnO nanofibers looked like interconnected balls with a rougher surface and a larger diameter than those of Zn-rt. This observation indicates that the PVP could maintain the scaffold of nanofibers and decomposed from Zn/PVP nanofibers by calcination. As the calcination temperature increased to 873 K, the ZnO particles of the internal parts of Zn-rt nanofiber could be observed and the diameter decreased due to the decomposition of PVP in the nanofibers. After reaching a higher calcination temperature, 1173 K, the ZnO crystals may be aggregated together, consequently, the diameter of Zn-1173 increased more, comparing with that of Zn-873. Therefore, the diameter and morphology of the ZnO are strongly dependent on the calcination temperature.

XRD Analysis. In order to investigate the crystalline phase and the function of the calcination temperature for the nanofibers, the XRD patterns of Zn-rt, Zn-873, and Zn-1173 were taken and shown in Figure 2. The diffraction pattern of Zn-rt shows no characteristic diffraction. This implies that the Zn-rt nanofibers have amorphous and polymeric properties. As the calcination temperature increased to 873 and 1173 K, all apparent diffraction peaks confirmed the formation of the pure hexagonal close packed (hcp) ZnO phase with high crystallinity.[24] The observed XRD patterns of Zn-1173 have sharper and stronger peak intensity than those of Zn-873. The average crystallite size of ZnO nanofibers was deduced with (101) peak at $2\theta = 36.25^{o}$ using the well known Debye-Scherrer's equation.[25] The calculated average crystal sizes of Zn-873 and Zn-1173 are 24.98 (± 1.13) nm 43.69 (± 1.73) nm, respectively. These observations suggest that the calcination process can play a role to remove the PVP from Zn-rt nanofibers and improve the crystallinity of ZnO nanomats. Moreover, as the calcination temperature increased from 873 to 1173 K, the crystal size in calcined nanomats becomes larger due to the aggregation of each nanoparticle in ZnO nanofibers. These results are in agreement with SEM observation.

TEM Analysis. For further investigation of the effect of calcination temperature on the ZnO nanomats, TEM images of Zn-1173 were collected as shown in Figure 3. The Figures

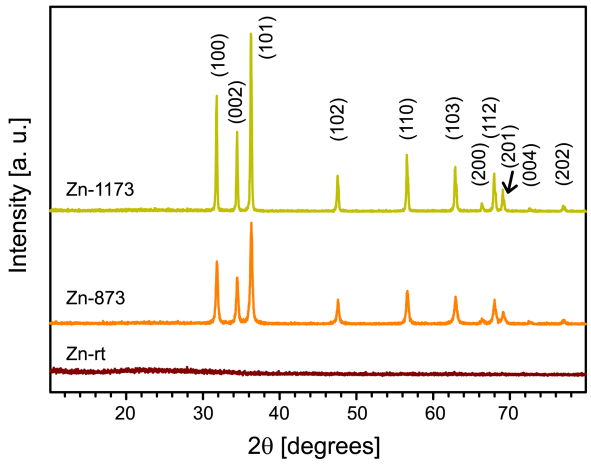

Figure 2. The XRD patterns of the Zn/PVP nanofibers (Zn-rt) and ZnO nanofibers calcined at different temperatures (Zn-873 and Zn-1173).

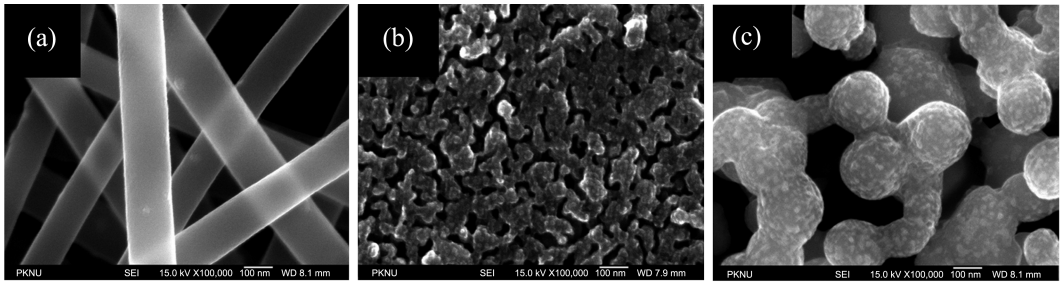

Figure 1. The SEM images of ZnO nanofibers of (a) Zn-rt, (b) Zn-873, and (c) Zn-1173. The size of scale bar in the figure is 100 nm.

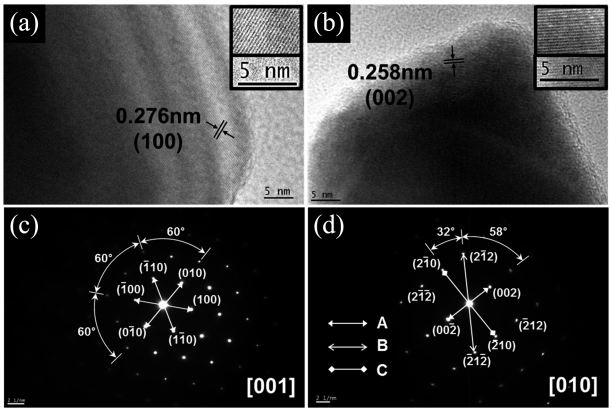

Figure 3. The high resolution TEM images at (a) and (b) and the selected area electron diffraction (SAED) patterns at (c) and (d) of Zn-1173 nanofibers.

3(a) and (b) show high resolution TEM images taken at different sites of Zn-1173 nanomats which show parallel arrangement revealing the crystallinity of ZnO nanomats. The regular lattice fringes of Figure 3(a) and (b) were approximately 0.28 (± 0.07) and 0.26 (± 0.08) nm, respectively. Those values correspond to the hcp ZnO of (100) and (002) plane, respectively. The Figures 3(c) and (d) show the selected area electron diffraction (SAED) patterns indexing [001] and [010] directions of the hexagonal wurtzite ZnO structure. SAED results were also confirmed the crystalline structure of the ZnO nanofibers calcined at 1173 K.[26] This observation clearly matched with the d-spacing of the XRD results of the ZnO.[24] It could explain that the crystallinity of the ZnO nanofibers is developed by the calcination process.

XPS Analysis. The chemical environment of the ZnO nanofibers was examined with XPS. As the calcination temperature increased Zn 2p peaks were pronounced and the characteristic peak of PVP, N 1s peak, was diminished shown in Figure 4. The C 1s peak was decreased by calcination at high temperatures as well. Even though the calcination system was evacuated during calcination, the decomposed carbon species from PVP was partially re-deposited on the

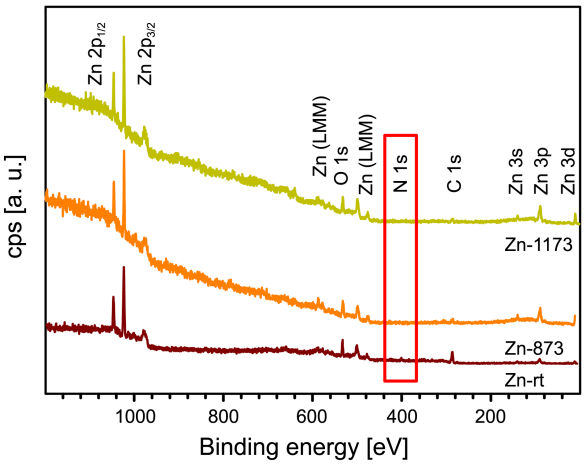

Figure 4. XPS Survey spectra of ZnO nanofibers of Zn-rt, Zn-873, and Zn-1173.

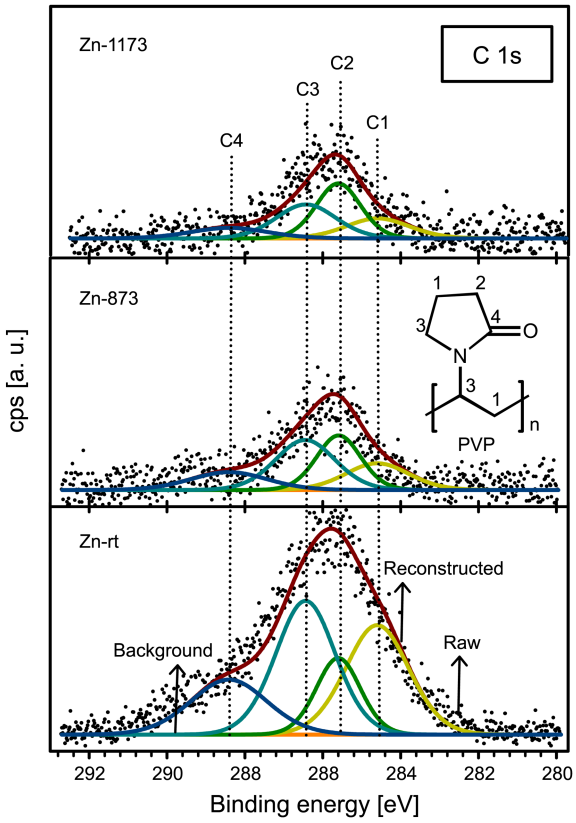

Figure 5. The deconvoluted high resolution the C 1s XPS spectra of Zn-rt and ZnO nanofibers calcined at 873 and 1173 K. (inset is molecular structure PVP)

surface region of the ZnO nanomats. This might be the cause of the existence of carbon species on the nanofibers.

The detailed binding energies of carbon species were assigned after the deconvolution process with high-resolution XPS spectra of C 1s binding energy region. All XPS spectra shown here were referenced with adventitious carbon at 284.6 eV.[28] The chemical structure of PVP was shown in the inset of Figure 5. The labels shown in the chemical structure assigned from low to high binding energy side depending on the chemical environment of the carbon. The four deconvoluted C 1s peaks were assigned to the carbons as C-C (denoted as C1, 284.6 ± 0.1 eV), C-C=O (C2, 285.6 ± 0.1 eV), C-N (C3, 286.4 ± 0.1 eV), and C=O (C4, 288.4 ± 0.1 eV). The atomic ratio of C1:C2:C3:C4 of Zn-rt was 2.04:1.00:2.35:1.24 which is close to the ratio of carbon species in PVP. As calcination temperature increased, the total intensity of carbon species decreased and the ratio among carbon species with different oxidation states changed. The peak intensities of C1, C3, and C4 drastically decreased due to the decomposition of PVP from the ZnO nanofibers. However, the C2 intensity did not change much. The re-deposited carbon species on the ZnO nanofiber might exist as a carbonyl species. This observation is quite consistent with the O1s XPS results shown in Figure 6(a). The N 1s peak was disappeared after calcination at high temperarture (not shown here). This implies that the PVP in the nanofibers was decomposed after calcination.

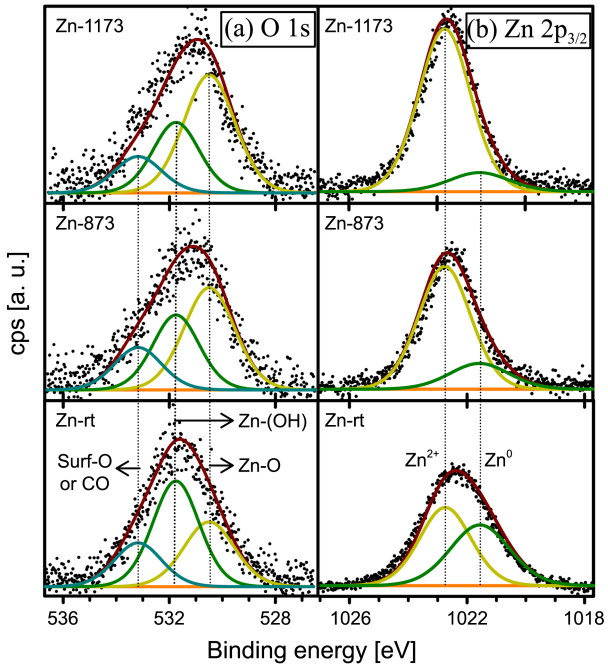

Figure 6. Representative XPS spectra of (a) O 1s and (b) Zn $2p_{3/2}$ of as electospun nanofibers and ZnO nanofibers calcined at 873 and 1173 K.

The deconvoluted high resolution O 1s and Zn $2p_{3/2}$ XPS spectra are shown in Figures 6(a) and (b), respectively. Due to the large spin-orbit coupling constant of Zn 2p (23.1 eV), Zn $2p_{3/2}$ peak was deconvoluted and shown in the figure for clarity. Three oxidation states for oxygen and two oxidation states for zinc were assigned after peak deconvolution. The assigned binding energies of O 1s are Zn-O (530.5 ± 0.1 eV), Zn-(OH) (531.7 ± 0.1 eV), and Surf-O/CO (533.1 ± 0.1 eV). The assigned binding energies of Zn $2p_{3/2}$ are centered at 1021.5 ± 0.1[29] and 1022.7 ± 0.1 eV for Zn^0 and Zn^{2+}, respectively. The assigned binding energies of O 1s and Zn $2p_{3/2}$ are in agreement with the previously reported values.[30,31]

As shown in Figure 6, thermal oxidation of zinc was observed by calcination of ZnO nanofibers. The atomic contents of Zn^0 and Zn^{2+} in Zn-rt were 47.3 and 52.7 at.%. After calcination of ZnO nanomats at 1173K, the atomic contents of Zn^0 and Zn^{2+} changed to 88.1 and 11.9 at.%, respectively. The thermal oxidation of Zn was easily established by calcination.[32] The contents of Surf-O/CO were almost constant as 20.2, 18.9, and 15.7 at.% for Zn-rt, Zn-873, and Zn-1173, respectively. These phenomena could indirectly explain the existence of re-deposited carbonyl species on the ZnO nanomats after calcination. However, the ratios of $Zn(OH)_2$ to ZnO in Zn-rt, and Zn-1173 (Figure 6(a)) were converted from 47.7:32.1 to 29.7:54.6. That ratios were deduced after deconvolution of O 1s peak. This might have happened because the hydroxide species could have decomposed and evaporated as H_2O during the calcination process. The total amount of oxygen bound with Zn^{2+} (ZnO and $Zn(OH)_2$) were 79.8, 81.1, and 84.3 at.% in Zn-rt, Zn-873, and Zn-1173, respectively. The increased amounts of oxygen and Zn^{2+} from Zn-rt to Zn-1173 are 4.5 and 35.4 at.%, respectively. After careful consideration of atomic sensitivity factors of O 1s (0.63) and Zn 2p (5.3),[28] the deduced chemical formula was $Zn_{6.68}O_{7.14}$ which is close to the stoichiometric compound, ZnO.

Conclusion

In conclusion, the diameter of calcined ZnO nanofibers increased as the calcination temperature increased. And the total intensity of the carbon species decreased due to the decomposition of PVP in the nanofiber as the calcination temperature increased. In addition, as the effects of calcination temperature on the oxidation states of ZnO is still not well documented in other literatures, we used the XPS to characterize and identify the thermal oxidation of Zn species in the ZnO nanofibers. The initial ZnO nanofibers contained the two oxidation states, Zn^0 and Zn^{2+} in almost equal amounts. However, as the calcination temperature increased, the amount of Zn^{2+} amply increased while Zn^0 decreased. This means that the calcination promoted the oxidation of Zn species.

Acknowledgments. This research was supported by Basic Science Research Program through the National Research Foundation of Korea (NRF) funded by the Ministry of Education, Science and Technology (2011-0026585).

References

1. Liu, L.; Li, S.; Zhuang, J.; Wang, L.; Zhang, J.; Li, H.; Li, Z.; Han, Y.; Jiang, X.; Zhang, P. *Sen. Act. B* **2011**, *155*, 782.
2. Yiquan, W.; Zexuan, D.; Nathan, J. J.; Robert, L. C. *Mater. Lett.* **2011**, *65*, 2683.
3. Yang, M.; Xie, T.; Peng, L.; Zhao, Y.; Wang, D. *Appl. Phys. A* **2007**, *89*, 427.
4. Song, J. H.; Wang, X. D.; Liu, J.; Liu, H. B.; Li, Y. L.; Wang, Z. L. *Nano Lett.* **2008**, *8*, 203.
5. Park, D.; Tak, Y.; Kim, J.; Yong, K. *Surf. Rev. Lett*. **2007**, *14*, 1061.
6. Sun, Z. P.; Liu, L.; Zhang, D. Z. *Nanotechnology* **2006**, *17*, 2266.
7. Bagci, V. M K.; Gulseren, O.; Yildirim, T.; Gedik, Z.; Ciraci, S. *Phys. Rev. B* **2002**, *66*, 045409.
8. Liao, L.; Lu, H. B.; Li, J. C.; Liu, C.; Fu, D. J.; Liu, Y. L. *Appl. Phys. Lett.* **2007**, *91*, 173110.
9. Xu, W. Z.; Ye, Z. Z.; Ma, D. W.; Lu, H. M.; Zhu, L. P.; Zhao, B. H.; Yang, X. D.; Xu, Z. Y. *Appl. Phys. Lett.* **2005**, *87*, 093110.
10. Qi, Q.; Zhang,, T.; Wang, S.; Zheng, X. *Sens. Act. B Chem*. **2009**, *137*, 649.
11. Spinolo, G.; Ardizzone, S.; Trasatti, S. *J. Electroanal. Chem.* **1997**, *423*, 49.
12. Jung, B. O.; Kim, D. C.; Kong, B. H.; Lee, J. H.; Lee, J. Y.; Cho, H. K. *Eletrochem. Sol. St. Lett.* **2011**, *14*, H446.
13. Noguchi, S.; Mizuhashi, M. *Thin Solid Films* **1981**, *77*, 99.
14. Liu, Y.; Mi, C.; Su, L.; Zhang, X. *Electrochim. Acta* **2008**, *53*, 2507.
15. Dan, L.; Younan, X. *Adv. Mater*. **2004**, *16*, 1151.
16. Ramaseshan, R.; Sundarrajan, S.; Jose, R.; Ramakrishna, S. *J. Appl. Phys.* **2007**, *102*, 111101.
17. Hu, C. C.; Cheng, C. Y. *Electrochem. Solid-State Lett.* **2002**, *5*, A43.
18. Ding, B.; Ogawa, G.; Kim, J.; Fujimoto, K.; Shiratori, S. *Thin Solid Films* **2008**, *516*, 2495.

19. Park, J. A.; Moon, J.; Lee, S. J.; Lim, S. C.; Zyung, T. *Curr. Appl. Phys.* **2009**, *9*, S210.
20. Venugopal, J.; Ramakrishina, S. *Appl. Biochem. Biotech*. **2005**, *125*, 147.
21. Wu, Y.; Dong, Z.; Jenness, N. J.; Clark, R. L. *Mater. Lett.* **2011**, *65*, 2683.
22. Sangkhaprom, N.; Supaphol, P.; Pavarajarn, V. *Ceram. Intern*. **2010**, *36*, 357.
23. Jo, J. M.; Park, J.; Kim, D.; Koh, S. W.; Kang, Y. C. *Bull. Korean Chem. Soc.* **2010**, *31*, 1776.
24. JCPDS Database, International Center for Diffraction Data 1997, PDF 80-0075.
25. Klong, H. P.; Alexander, L. E. *X-ray Diffraction Procedures for Crystalline and Amorphous Materials*; Wiley: New York, 1954; pp 491-538.
26. Wang, Y.; Zhong, Z.; Chen, Y.; Ng, C. T.; Lin, J. *Nano Res*. **2011**, *4*, 695.
27. Espitia-Cabrera, I.; Orozco-Hernandez, H. D.; Bartolo-Perez, P.; Contreras-Garcia, M. E. *Surf. Coat. Technol.* **2008**, *203*, 211.
28. Wagner, C. D.; Riggs, W. M.; Davis, L. E.; Moulder, J. F.; Muilenberg, G. E. *Handbook of X-ray Photoelectron Spectroscopy*; Perkin-Elmer Corp.: USA. 1979.
29. Islam, M. N.; Ghosh, T. B.; Chopra, K. L.; Acharya, H. N. *Thin Solid Films* **1996**, *280*, 20.
30. Sepulveda Guzman, S.; Reeja-Jayan, B.; Rosa, E.; Torres-Castro, A.; Gonzalez Gonzalez, V.; Jose-Yacaman, M. *Mater. Chem. Phys*. **2009**, *115*, 172.
31. Shiva, H.; Nilima, H.; David, L.; Bruce, C. *Nanoscale Res. Lett.* **2009**, *4*, 1421.
32. Guo, C. F.; Wang, Y.; Liu, Q. *J. Nanosci. Nanotechno*. **2010**, *10*, 1.